ACS BIO & MED CHEM Au
AN OPEN ACCESS JOURNAL OF THE AMERICAN CHEMICAL SOCIETY

pubs.acs.org/biomedchemau

Article

Live-Cell SOFI Correlation with SMLM and AFM Imaging

Riley B. Hargreaves, Sam Duwé, Ashley M. Rozario, Alison M. Funston, Rico F. Tabor, Peter Dedecker, Donna R. Whelan,* and Toby D. M. Bell*

Cite This: *ACS Bio Med Chem Au* 2023, 3, 261−269

Read Online

ACCESS | Metrics & More | Article Recommendations | Supporting Information

ABSTRACT: Standard optical imaging is diffraction-limited and lacks the resolving power to visualize many of the organelles and proteins found within the cell. The advent of super-resolution techniques overcame this barrier, enabling observation of subcellular structures down to tens of nanometers in size; however these techniques require or are typically applied to fixed samples. This raises the question of how well a fixed-cell image represents the system prior to fixation. Here we present the addition of live-cell Super-Resolution Optical Fluctuation Imaging (SOFI) to a previously reported correlative process using Single Molecule Localization Microscopy (SMLM) and Atomic Force Microscopy (AFM). SOFI was used with fluorescent proteins and low laser power to observe cellular ultrastructure in live COS-7 cells. SOFI-SMLM-AFM of microtubules showed minimal changes to the microtubule network in the 20 min between live-cell SOFI and fixation. Microtubule diameters were also analyzed through all microscopies; SOFI found diameters of 249 ± 68 nm and SMLM was 71 ± 33 nm. AFM height measurements found microtubules to protrude 26 ± 13 nm above the surrounding cellular material. The correlation of SMLM and AFM was extended to two-color SMLM to image both microtubules and actin. Two target SOFI was performed with various fluorescent protein combinations. rsGreen1-rsKAME, rsGreen1-Dronpa, and ffDronpaF-rsKAME fluorescent protein combinations were determined to be suitable for two target SOFI imaging. This correlative application of super-resolution live-cell and fixed-cell imaging revealed minimal artifacts created for the imaged target structures through the sample preparation procedure and emphasizes the power of correlative microscopy.

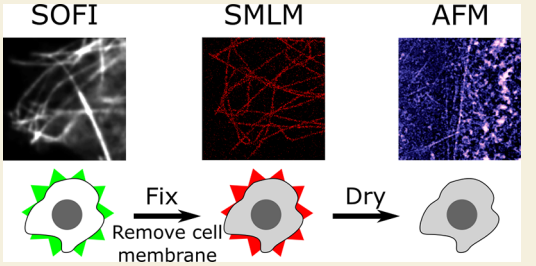

KEYWORDS: *super-resolution, intensity fluctuation, reversibly switchable fluorescent proteins, microtubules, actin, mitochondria, multi-tau*

INTRODUCTION

Fixation of cells prior to imaging is useful and convenient and has been used with great success for many decades. However, fixation can cause changes, and thus the sample no longer completely represents the biology of the system at the moment of fixation. These changes can be acceptable so long as the target of interest is not perturbed or the labeling of said target is not affected or inaccurate as a result.[1,2] That fixation (chemical or otherwise) causes changes is a well-known problem, and much has been done to understand, quantify, and minimize such effects.[3] Live imaging avoids these issues but is harder to perform and restricts labeling options, since immunolabeling cannot be used because antibodies are unable to cross the cell membrane and label targets. Different approaches are required to label internal structures in live cells with the use of fluorescent proteins (FPs) being one of the most common.[4,5] However, labeling a target with an FP can still create changes to the sample, and so careful validation and interpretation of these live imaging results are still important. A combination of live-cell and fixed-cell imaging is a method through which live experiments can "validate" the fixation approach, while fixed methods are used for the majority of the investigation. This has been performed to great effect investigating the transport of cargo along microtubules,[6] capturing the movement of target structures in live cells followed by fixation and super-resolution imaging of microtubules through SMLM to determine the structure of the microtubule network being followed. Applying this validation with diffraction limited imaging is relatively straightforward, since each imaging method operates at a similar resolution; however when utilizing super-resolution methods in fixed cells there can be greater artifactual detail, and it becomes challenging to perform a direct comparison with live-cell imaging.

We[7] and others[8−10] have recently showed that super-resolution and AFM can be performed correlatively to provide contextual information via topographical mapping to target structures imaged under super-resolution. Various super-resolution techniques have been combined with AFM, including structured illumination microscopy (SIM)[11] and stimulated emission depletion microscopy (STED).[12] SMLM has also been used correlatively by Hirvonen et al. to investigate podosome

Received: December 29, 2022
Revised: March 9, 2023
Accepted: March 10, 2023
Published: March 28, 2023

https://doi.org/10.1021/acsbiomedchemau.2c00086
ACS Bio Med Chem Au 2023, 3, 261−269

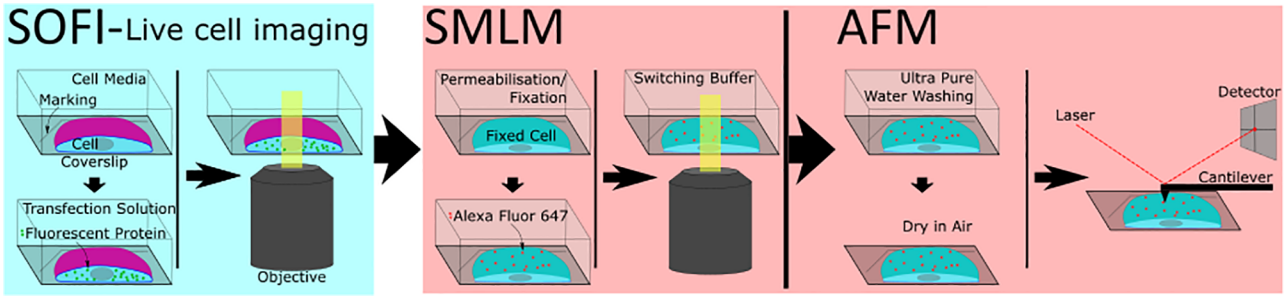

Figure 1. New three step correlative pipeline with live-cell super-resolution added to the beginning of the previous method.[7] Seeded cells are first transfected with a DNA plasmid, expressing a fluorescent protein within the living cell. Once enough fluorescent protein has been expressed, the coverslip is taken to be imaged. The cell can then be fixed and membrane (magenta) removed to ensure no major structural rearrangement from natural processes. Antibody labeling can be performed and the cell imaged again to determine the effects of permeabilization and fixation on the internal structures. Finally the sample is washed extensively with ultrapure water and dried in ambient conditions before being imaged on AFM to produce a topographical map. Figure adapted with permission from ref 7. Copyright 2022 IOP Publishing.

structure[13] and by us, where we showed complementary information from SMLM and AFM could determine more accurate microtubule widths and arrangements, providing a more complete picture of the microtubule network.[7] More work by Bondia et al. has also combined AFM with two-color SMLM, using quantum dot-functionalized β-lactoglobulin amyloid-like fibrils to observe the emission properties and distribution of the quantum dots via SMLM and the topography and filament structure of the fibrils via AFM.[14] By front-loading live-cell super-resolution imaging to this correlative pipeline, a picture of the cell prior to fixation can be obtained and changes occurring as a result of fixation can be determined.

Live-cell imaging is difficult to perform with super-resolution, but some approaches have proved to be successful.[15] SIM and STED have been used in live systems with ∼50−100 nm resolutions,[16,17] while SMLM approaches using reversibly switching fluorescent proteins (RSFPs)[18] or caging systems[19] have also been explored. A number of requirements need to be considered when selecting a method for live/fixed-cell correlative imaging. These include the speed of image acquisition, the convenience of imaging, and the additional sample preparation required. A faster image acquisition will minimize the time between the live measurement and the sample getting fixed. The ability to perform live-cell imaging on the same microscope as fixed-cell imaging aids with observing the same target for correlation. Avoiding additional sample preparation can preserve biological relevance. Maximizing the resolution increase is also challenging to do for live imaging, as the cell must be kept healthy for the duration of acquisition to image in as natural a state as possible. Most super-resolution methods that achieve below 50 nm resolution such as SMLM, STED, and SIM require high laser power which can lead to phototoxicity issues. Live-cell super-resolution optical fluctuation imaging (SOFI) can be achieved on the same microscope as SMLM and gives a moderate resolution increase of 2−3×, and while it requires RSFPs it does not require any additional preparation beyond transfection of appropriate plasmids.[20−22]

SOFI requires the coexpression of appropriate RSFPs such as Dronpa[23] or rsGreen1. Photoswitching of the RSFPs can be induced at low laser powers which avoid causing significant phototoxicity.[24,25] The fluctuations caused by the photoswitching of the RSFPs are detected on a EMCCD camera and then post-processed to generate the super-resolved image at a resolution of ∼120−150 nm in x and y for second-order SOFI.[26] This live-cell technique can be added to the SMLM-AFM procedure to provide a live-cell reference for fixed-cell imaging. Recent developments of SOFI have extended this imaging into 3 dimensions by separating different focal planes within the sample and collecting them on either separate detectors or different regions of the same detector.[27,28] This has resulted in correlation of 3D SOFI with scanning ion-conductance microscopy (SICM),[29] another method of measuring topography, in live-cells. Self-blinking dyes,[30] which spontaneously switch between a fluorescent "on" state and dark "off" state, were utilized to perform two-color 3D SOFI of actin and microtubules with correlative SICM topography on fixed cells. Single color live-cell correlative SOFI/SICM imaging of actin was also performed through transfection of DNA plasmids to express actinin-mEOs-2 for time-lapse experiments.

Multicolor SMLM can image multiple separate targets through labeling them with different color emitters, separating them by their absorption and/or emission wavelengths. This allows for the interactions between structures to be investigated and the possibility of extending the correlative pipeline to multitarget imaging. However, a current limitation in implementing two color SOFI is that the majority of suitable RSFPs emit at similar wavelengths in the green part of the spectrum and are not easily separated by spectral filtering.[31] Where multicolor imaging is possible in SMLM with different color emitters a different method of differentiation is required for SOFI. Multi-tau SOFI was developed by Duwé et al. to separate similar color FPs based on their blinking kinetics, with a wider difference in blinking speed leading to easier separation of FPs.[32] The acquisition of data is the same as for single target SOFI imaging, but postprocessing takes the fluorescence fluctuations and separates the FPs based on the rate with which they blink. This enables the imaging of multiple targets through the correlative imaging method, providing subdiffraction insights within the live cell.

Here, we optimized and tested the full correlative approach from live to fixed-cell super-resolution imaging and topographical mapping, i.e., SOFI through SMLM to AFM. We determined the changes which occur to the microtubule network as a result of removing the cellular membrane through application of Triton X-100. Analysis of microtubule widths across all three microscopies was conducted to compare each technique. Finally, correlation of two color SMLM with AFM was performed with the potential of extending this multitarget correlation to live-cell imaging through application of two-target multi-tau SOFI.

https://doi.org/10.1021/acsbiomedchemau.2c00086
ACS Bio Med Chem Au 2023, 3, 261−269

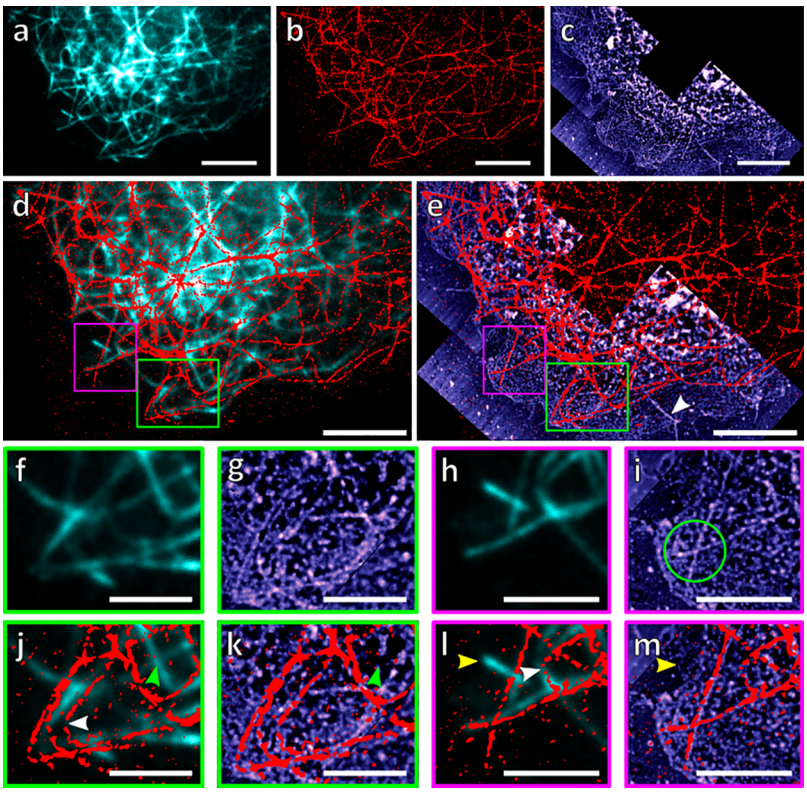

Figure 2. Same cell imaged under SOFI using pMAP4-N1-ffDronpa, SMLM with Alexa Fluor 647 and AFM. (a) shows the original SOFI image, (b) is the SMLM image of the same region after membrane removal and antibody labeling. (c) is the AFM image of the same region. (d) is the overlaid SOFI/SMLM image comparing the microtubule network. (e) shows the overlaid microtubule network from SMLM on the topographical map from AFM. (f,g,j,k) are a zoom in of a cluster of microtubules outlines with a green box. The green arrowhead indicates a microtubule that appears on SOFI but is not shown on SMLM or AFM. (h,i,l,m) are a zoom in of a microtubule intersection outlined with a purple box. The yellow arrowhead indicates another microtubule present in live-cell SOFI but not shown under either SMLM or AFM. Scale bars for (a−e) and (f−m) are 5 and 2 μm, respectively.

RESULTS AND DISCUSSION

The flowchart shown in Figure 1 explains the experimental steps used throughout the correlative imaging process. Cells are cultured onto a coverslip scratched with a distinctive mark to facilitate locating the same cell across different imaging sessions. The cells are then transfected with a DNA plasmid to label the target structures with the required fluorescent protein and left to transfect for 24 h. Once the cells are expressing the fluorescent proteins they are taken to the microscope to be imaged in 37 °C PBS, upon location of the distinctive mark, cells nearby were mapped and imaged with SOFI. Immediately following collection of data of the live cell for SOFI, the sample was fixed. This cellular membrane removal and fixation process was optimized previously in our laboratory.[7] In summary, surfactant is carefully used to remove much of the cellular membrane while preserving the structure of the cellular cytoskeleton enabling access of the cantilever to internal structures. Once the cells have been fixed and immunolabeled they are then imaged first for SMLM and then for AFM.

Some initial experiments were conducted adjusting the time that cells were left transfecting with DNA plasmids before SOFI imaging was performed; these and all subsequent SOFI images are generated at second order cumulant. These included transfection 24 h before imaging and 48 h before imaging. A double transfection, with first transfection 48 h before imaging and a repeat transfection 24 h before imaging, was also tested. It was determined that the single 24 h transfection was sufficient to produce clean SOFI images and was used for the subsequent experiments. Analysis of microtubule widths from these SOFI images were determined to be 304 ± 55 nm and 221 ± 36 nm for the 24 h and 48 + 24 h transfections. Details on the imaging and analysis can be found in the Supporting Information (Figure S1) along with example raw acquisition fluctuation data in the form of video (Video 1 and 2). Once SOFI imaging of microtubules was successful, correlation with SMLM and AFM was performed.

Figure 2 compares the microtubule network before the membrane removal and fixation process with SOFI (a), and after this process with SMLM (b) and AFM (c). The sample was imaged for SOFI, and immediately following data acquisition the sample was removed from the microscope and the membrane removal and fixation procedure was started. Once the sample was fixed and stained it was imaged using SMLM, after which the sample was washed with ultrapure water 3 times and left for 4 h to dry in ambient conditions before being imaged on the atomic force microscope.

The SMLM image in Figure 2b appears slightly discontinuous, which can be seen more clearly by the white arrowheads in (j) and (l). These could be caused by the RSFPs used for SOFI still being present on the microtubules, preventing complete coverage of the microtubules for antibody staining and potentially affecting height measurements obtained from AFM. This is shown in the Supporting Information (Figure S2), comparing Figure 2b with a cell without MAP4-N1-ffDronpa attached to the microtubules. With the correlative imaging still providing nearly complete coverage of the

https://doi.org/10.1021/acsbiomedchemau.2c00086
ACS Bio Med Chem Au 2023, 3, 261−269

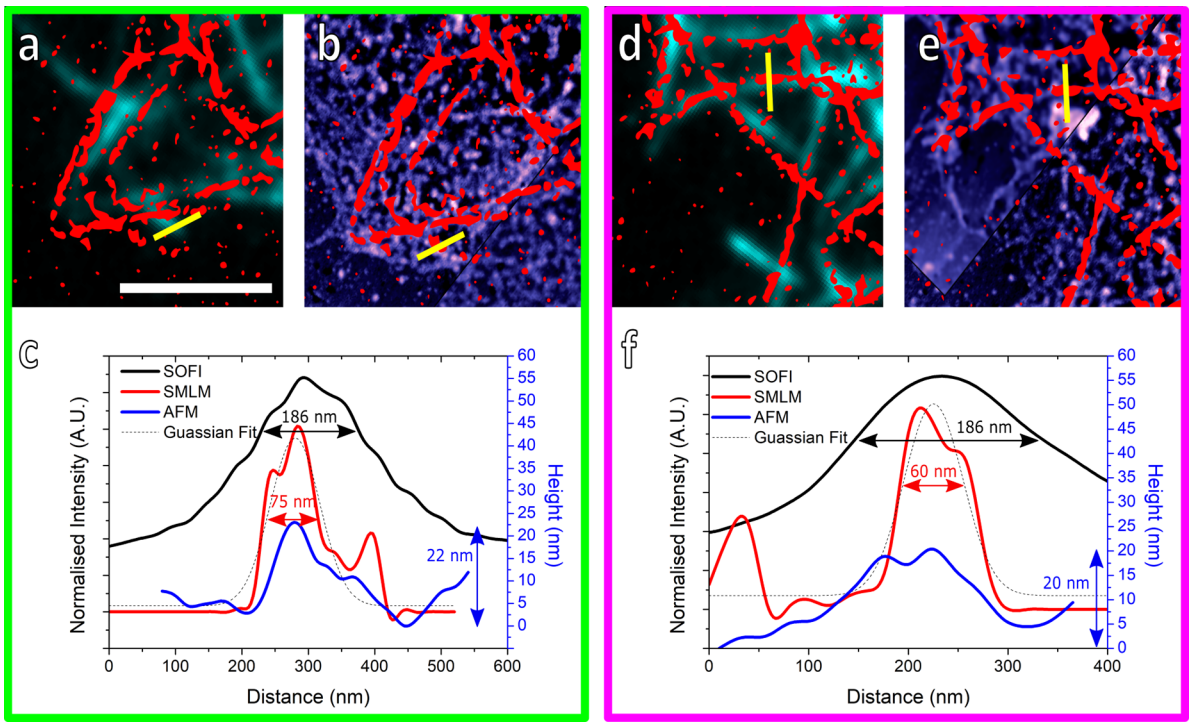

Figure 3. Widths of microtubules measured across the different imaging modes. The yellow lines in (a) (SOFI/SMLM) and (b) (SMLM/AFM) show the single microtubule widths measured in (c). (d) and (e) also show a microtubule with widths in (f). For SOFI and SMLM images, widths were calculated from fitting Gaussian curves to the intensity cross sections averaged over 100 nm sections and determining 2× their standard deviation. AFM widths were calculated from the measured height of the microtubule in relation to its surroundings. SOFI normalized intensity has been offset for clarity. Scale bar is 2 μm.

microtubule network, seen in Figure 2b,d this shows that both methods of staining can be performed on the same target.

The general shape of the microtubule network in the enlarged images (j,l) is consistent between live and fixed images, with the same extensive curvature observed in (j) and the two microtubules crossing each other in (l) indicating preservation of the structure through the membrane removal process. The time from finishing live-cell image acquisition to finishing fixation was approximately 20 min, which is enough time for some movement and polymerization/depolymerization of the microtubule network to occur, but not enough time for substantial rearrangement.[33] This is revealed in the comparison between pre and post fixation, Figure 2d, where some features of the network can be observed in both imaging modes while being slightly displaced or distorted. In particular, Figure 2f−m highlights two such regions, one where multiple microtubules start curving back on themselves and the other at a microtubule crossing point. These filament arrangements are observed both in live-cell imaging and after fixation, although there is some slight variation likely caused from the general microtubule dynamics of cells, such as the microtubule highlighted with the green arrowhead in (j) appearing under SOFI but absent in SMLM. This is potentially due to the microtubule moving slightly in the short period of time before fixation occurred, rearranging into the conformation shown in SMLM due to either natural biological processes or as an affect from the fixation procedure. Similarly, the yellow arrowhead in (l,m) shows another microtubule present in the SOFI image but absent in both SMLM and AFM, potentially depolymerizing in the time between live-cell imaging and fixation. This could also be a microtubule outside the SMLM imaging depth window of 0.5−1 μm while still being observed in the 2−3 μm depth window of epifluorescence or SOFI imaging. There are also filament structures visible in the AFM image which are not observed by either SMLM or SOFI, shown by the white arrowhead in (e). This structure, and others like it, could be actin or other intermediate filaments present within the cell but not fluorescently labeled.

Microtubule widths can also be determined from these images, allowing for comparisons between imaging techniques and the known microtubule diameter of 25 nm.[34] Figure 3 shows two such microtubules analyzed to determine their widths across the three imaging modes, as there are occasionally slight differences in the location of the microtubule between the live-cell imaging of SOFI and fixed imaging from SMLM and AFM, the yellow cross section shown on (a,d) was used for only SOFI analysis, SMLM and AFM widths were analyzed using the yellow cross sections on (b,e). Widths were calculated via Line Profiler[35] for SOFI and SMLM, by applying a Gaussian fit to the fluorescence intensity cross sections and finding 2× the standard deviation. For AFM, the height measurement of the filament in relation to its surroundings was obtained from the topographical cross section to determine the diameter.

The first microtubule measured in (a−c) showed the SOFI measurement to be much larger at 186 nm, when compared to the SMLM at 75 nm and the AFM at 22 nm. This measurement is consistent with the second microtubule measurement shown in (d−f), with SOFI finding a width of 186 nm, SMLM finding 60 nm and AFM 20 nm. The AFM measurements found an average height of 26 with a standard deviation of 13 nm (N = 39 from 3 cells) and were smaller than expected. Because these values were obtained by comparing the maximum height of the microtubule to the surrounding environment, microtubules embedded in the remains of the cell can give a measurement

https://doi.org/10.1021/acsbiomedchemau.2c00086
ACS Bio Med Chem Au 2023, 3, 261−269

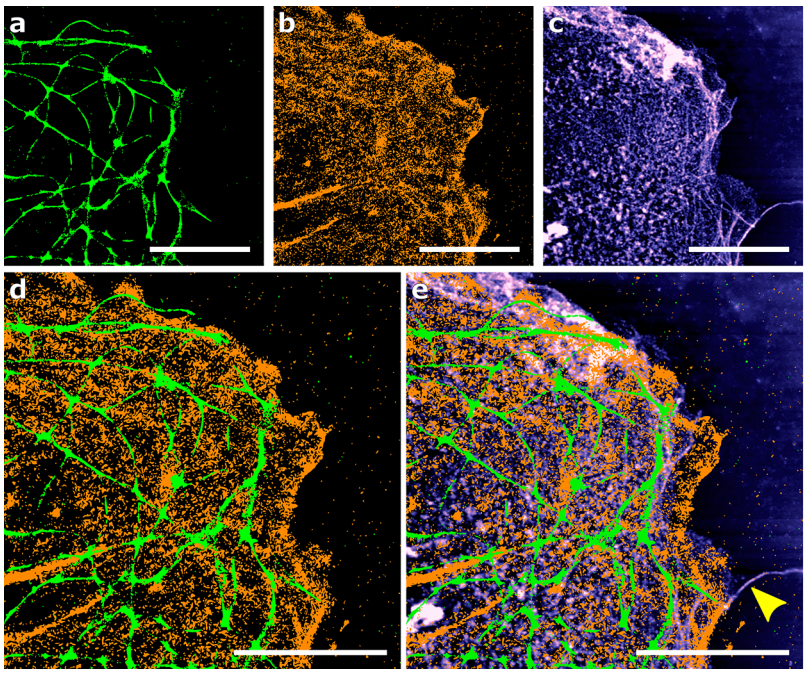

Figure 4. Two color correlative SMLM-AFM imaging of microtubules and actin. (a) shows the SMLM image of microtubules in green and labeled with anti-α-tubulin Alexa Fluor 532 while (b) shows the actin of the same region in orange labeled with Phalloidin Alexa Fluor 647. (c) is the AFM topographical map of the same region. (d) shows the two color SMLM image, with (a) and (b) overlaid. (e) has the multitarget SMLM image from (d) overlaid on the AFM topographical map (c), highlighting the microtubules (green) and actin (orange). Scale bars are 5 μm.

smaller than their true diameter. Average widths obtained from SOFI images were 249 $\pm$ 68 nm (N = 89 from 5 cells), which are much larger than both SMLM and the true value. This is likely due to the lower resolution second order SOFI gives in combination with the addition of MAP4 proteins and RSFPs to the microtubules, increasing their observed diameter. The increased resolution of SMLM obtains microtubule widths closer to the expected value, 71 $\pm$ 33 nm (N = 118 from 3 cells), but still slightly larger. This could be due to the localization precision of each PSF Gaussian fit and addition of primary and secondary antibodies along with the dye molecule for staining. Statistical analysis of this data can be found in the Supporting Information (Figure S3).

We previously showed that microtubule intersections can be investigated to determine the arrangement of microtubules relative to each other,[7] and this analysis has been applied again for the intersection in Figure 2i within the green circle which can be found in the Supporting Information (Figure S4). This method determined the microtubule aligned horizontally in the image is passing above the microtubule aligned vertically. Microtubules act as an excellent beginning point for correlative imaging due to their consistent structure; however extending this protocol to other targets would allow the investigation of many different research topics.

Actin is important in the movement of organelles and maintaining cellular structure with filaments extending throughout the entire cell.[36] Due to its importance for biological function, actin has become the target of a multitude of super-resolution studies. New insights into the structure of the actin network have been found,[37] and protein organization with actin around podosome clusters have also been investigated.[38] This makes actin a very promising target for multicolor correlative imaging.

Extending the correlation of SMLM-AFM to target two separate structures can be achieved in a straightforward fashion, since multicolor staining and imaging is well established for SMLM, and no changes need to be made for AFM imaging. Figure 4 shows two target correlation of SMLM and AFM, with microtubules (green) and actin (orange) labeled. SMLM images were obtained sequentially with actin stained with phalloidin Alexa Fluor 647 imaged first, followed by microtubules stained with anti-α-tubulin Alexa Fluor 532. Image registration was performed using bUnwarpJ package in ImageJ and a calibration of 100 nm fluorescent Tetraspecks to align the colors into the two color image in (d), removing chromatic aberrations. This was then overlaid onto the AFM topographical map to give the correlated two color image (e). The actin network appears to extend from the cell border on the AFM which could be due to the larger structures slightly further into the cell obscuring the small actin filaments at or outside the border. This misalignment could also be caused from the drying of the sample for AFM imaging causing a small amount of shrinking in comparison to the wet SMLM imaging. There is also a filament extruding from the cell indicated by the yellow arrowhead in (e) which is not labeled by either the microtubule or actin staining. This could be due to the phalloidin staining of actin being more susceptible to the washing steps when outside the cell, or, more likely, this filament is not actin or a microtubule but a different intermediate filament which was not labeled.

While multicolor SMLM is well established most of the RSFPs suitable for SOFI are green, making multicolor imaging difficult to perform for live-cell SOFI. Duwé et al.[32] have recently shown that switching kinetics can be used to discriminate between two RSFPs with overlapping emission spectra. This allows multi-target correlation for SOFI-SMLM-AFM to be possible, enabling the investigation of organelle interactions.

Some preliminary single-target SOFI experiments were conducted to determine the suitability of different plasmids and RSFPs which can be found in Figure S3 in the Supporting Information. These targets included microtubules with different

https://doi.org/10.1021/acsbiomedchemau.2c00086
ACS Bio Med Chem Au 2023, 3, 261−269

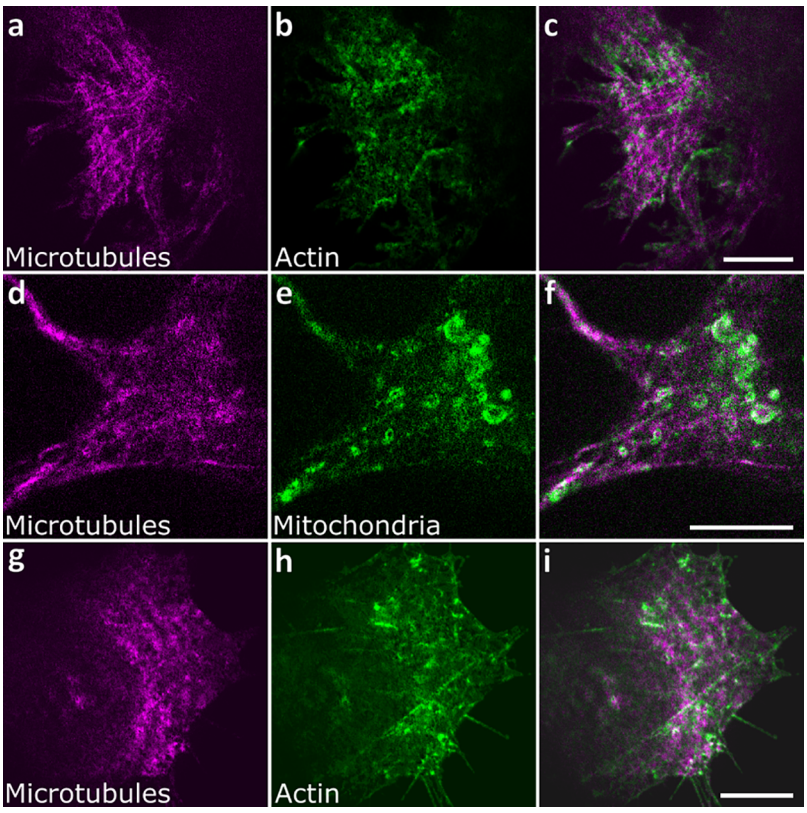

Figure 5. Multitarget SOFI of various structures with microtubules in magenta (faster blinking) and actin and mitochondria in green (slower blinking). (a−c) shows microtubules (pMAP4-N1-rsGreen1) (a), actin (pcDNA-lifeACT-rsKAME) (b), and the merged image (c), (d−f) shows microtubules (pMAP4-N1-rsGreen1) (d), mitochondria (pcDNA-DAKAP-Dronpa) (e), and the merged image (f). (g−i) shows microtubules (Tub-ffDronpaF) (g), actin (pcDNA-lifeACT-rsKAME) (h), and the merged image (i). Scale bars are 10 μm.

RSFPs, actin, and mitochondria due to their importance in cellular function.[39] Once these targets were established for single-target, they were then paired in various combinations for multitarget imaging.

Figure 5 shows three combinations of targets and fluorescent proteins used in multi-tau SOFI imaging. They were chosen to observe their performance for separation by their fluctuation kinetics. Duwé previously reported the fluctuation kinetics of various common fluorescent proteins,[32] and it was found that rsGreen1 and ffDronpaF had the fastest off-switching behavior and Dronpa and rsKAME had slower off-switching, enabling the pairing of a fast RSFP with a slow RSFP to be used for multi-tau SOFI. The combination with the largest separation was rsGreen1 and rsKAME, which can be seen in Figure 5a−c. While both rsGreen1/Dronpa (d−f) and ffDronpaF/rsKAME (g−i) RSFP combinations are slightly less separated, they still produced adequate multitarget images. The microtubules observed in (g) from Tub-ffDronpaF appear less specific than those using MAP4 to target microtubules. This signal could arise from free tubulin-FP units within the cytoplasm not incorporated into microtubules resulting in a lower labeling density on microtubules and higher background fluorescence. Because two separate plasmids need to be introduced into the same cell for dual expression, transfection rates for multi-tau SOFI are much lower than those needed for one target SOFI. This adds to the challenge in finding a cell expressing both RSFPs in a location which can be found again during a separate imaging session or different microscope for correlation. This could potentially be solved by encoding both targeting structure−RSFP combinations into the same expression plasmid. For long-term experiments, stably transfected cell lines could be developed by sorting cells with Fluorescence Activated Cell Sorting (FACS) to improve transfection rates.

CONCLUSION

In conclusion, we have developed correlative application of SOFI-SMLM-AFM to image microtubules first in live cells via SOFI and after cellular membrane removal and fixation with SMLM and AFM. The changes observed to the microtubule network between when live and following fixation were minimal indicating the SMLM imaging taken after membrane removal was still biologically relevant. There is a 20 min period between live-cell imaging and the end of fixation in which the microtubule network can shift and polymerize/depolymerise. One issue identified is that use of RSFPs for SOFI has potential to contribute to discontinuous MTs in SMLM images, likely due to restricting access of antibodies to binding sites on the MTs. This live-cell correlative approach has further validated the sample preparation method established for correlative SMLM-AFM of fixed cells with membrane removed, providing biological confidence.

Investigation of the microtubule widths across all microscopies revealed SOFI reporting the largest diameters of 249 ± 68 nm, which is still a 2−3-fold improvement over epifluorescence imaging. SMLM showed diameters of 71 ± 33 nm and AFM determined MTs protruded 26 ± 13 nm above the surrounding cellular material. These differences are due to the resolution limits of each technique and the labeling method used. Second order SOFI has the lowest resolution and when compounding with RSFP labeling which artificially increases the width of the

https://doi.org/10.1021/acsbiomedchemau.2c00086
ACS Bio Med Chem Au 2023, 3, 261−269

Table 1. Table of Each Plasmid Used within the Article, Detailing Their Name, What They Are Targeting, and What Fluorescent Protein Is Encoded

Plasmid Name	Encoding Target	FP	Backbone
pcDNA-DAKAP-Dronpa	mitochondrial membrane target DAKAP	Dronpa	pcDNA3 (Addgene vector database, 2092)
pcDNA-lifeACT-rsKAME	a 17 amino acid polypeptide that binds to actin (LifeAct)	rsKAME	pcDNA3 (Addgene vector database, 2092)
pMAP4-N1-rsGreen1	microtubule associated protein 4 (MAP4)	rsGreen1	pEGFP-N1 (EGFP gene removed) (Addgene vector database, 2491)
pMAP4-N1-ffDronpa	microtubule associated protein 4 (MAP4)	ffDronpa	pEGFP-N1 (EGFP gene removed) (Addgene vector database, 2491)
Tub-ffDronapF	tubulin subunit (Tub)	ffDronpaF	

microtubules, leads to these large microtubule diameters. SMLM has much better resolution; however the use of primary and secondary antibodies, along with the fluorescent dye will also increase the width of the microtubule observed. AFM has excellent height resolution; however to measure the filaments the local maximum is used, which can be obscured slightly if the microtubule is partially embedded in the surrounding environment.

Two target correlative SMLM-AFM imaging was performed on microtubules and actin, revealing that the actin filaments persist following membrane removal. The actin observed in SMLM did not appear to align perfectly with the AFM image, potentially due to drying of the sample for AFM image causing the cell to shrink slightly. The potential for two target correlative live-cell super-resolution imaging was explored with multi-tau SOFI, where it was determined that fluorescent protein combinations of rsGreen1-rsKAME, rsGreen1-Dronpa and ffDronpaF-rsKAME are suitable to be distinguished by their fluctuation kinetics.

This live-cell correlative imaging could be applied to investigate the changing structure of the cytoskeleton by using SOFI imaging to generate time lapse movies before fixation of the sample and investigating at better resolution with SMLM. Extending the two color correlation to SOFI as well would broaden the range of topics which can be investigated, enabling the imaging of two targets in a live cell, for example to observe potential interactions. Increasing the range of imaging targets available through cellular unroofing, especially for SOFI with the RSFP combinations that can be used for multi-tau, would complement the extension to multitarget correlative imaging. Utilizing 3-dimensional SMLM imaging could complement the topographical information obtained from AFM, providing greater z-information on target structures.

EXPERIMENTAL SECTION

Cell Culture and Seeding for Fluorescence Imaging

COS-7 (african green monkey kidney fibroblast-like, ATCC CRL1651) cells were cultured in Dulbecco's modified Eagle's medium (DMEM - high glucose) combined with 10% (v/v) fetal bovine serum and 1% (v/v) antibiotic/antimycotic (Sigma-Aldrich, A5955) and stored in 37 °C, 5% CO_2 humid incubator. Cells were passaged twice a week in 25 cm^2 flasks to maintain 40−90% confluency. For imaging, cells were seeded onto high precision coverglasses in 12 well plates following a previously outlined method.[7]

Transfection of DNA Plasmids for SOFI

For live-cell imaging, cells were seeded onto high precision (0.17 mm ±5 μm #1.5HP) 18 mm round coverglasses scratched with a carbide pen in a 12 well plate and grown to 60% confluence before transfection. Seeded cells were transfected using Fugene HD Transfection Kit according to the manufacturer's instructions (Promega). For each well, transfection media consisted of 1000 ng DNA plasmid (plasmids used can be found in Table 1 below) and 2 μL Fugene reagent in 100 μL DMEM was added to 1 mL complete media. Cells were incubated in transfection media for at least 24 h prior to imaging.

For transfection of multiple plasmids in a single well, 500 ng of each DNA plasmid was used with 2 μL Fugene reagent in 100 μL DMEM before addition to 1 mL complete media and incubation for at least 24 h before imaging.

Fluorescence Microscope Setup

SOFI and SMLM were performed on a previously described[7] home-built single molecule super-resolution microscope setup (Olympus IX81, 1.49 NA 100× TIRF objective, Andor iXon EM-CCD). Fluorescent proteins (rsKAME, rsGreen1, Dronpa, ffDronpa) were captured in the blue channel (200 mW Toptica 488 nm laser excitation, 525/50 bandpass emission filter), Alexa Fluor 532 was captured in the green channel (300 mW Dragon Lasers 532 nm, 570/50 bandpass emission filter) and Alexa Fluor 647 was captured in the red channel (500 mW Oxxius 638 nm laser excitation, 700/75 bandpass emission filter). For quick scanning to find marked areas, a 0.80 NA 20× objective was used. Image acquisition parameters were controlled using Micromanager.[40] Epifluorescence imaging was performed at 10 Hz (100 ms exposure) while navigating the sample. Wide-field illumination was used for epifluorescence and SOFI imaging while HiLo (quasi-TIRF) was used for SMLM acquisition.

SOFI Imaging

Cells were taken from the incubator and washed twice with warm PBS (37 °C) before being taken to the fluorescence microscope. Cells were imaged in warm PBS and scanned near the area of the scratch using ∼5−10 mW/cm^2 488 nm laser until cells expressing the fluorescent protein were found and epifluorescence imaged. To induce the photoswitching of the fluorescent proteins required for SOFI imaging, 50 mW/cm^2 488 nm laser excitation was used before capturing the area at 20 Hz (50 ms exposure) for 2000 frames.

Raw videos were analyzed in Igor Pro 7 using the Localizer package[41] under the SOFI tab. The parameters used for analysis were Order = 2, Pixel Combos = More, Also Average Image = checked, Frames per Image = 500. This produced an average image combining the analyzed frames which is representative of a diffraction limited fluorescence image and the SOFI image. Afterward, a deconvolution was applied using the settings Standard Deviation of the PSF = 1.6 pixels and Number of Iterations = 2. After rendering, images were optimized for display contrast. All SOFI images were created using second order cumulant SOFI.

Correlative SMLM/AFM Fixation and Imaging

Cells were fixed and imaged using a previously established method for correlative SMLM/AFM imaging.[7] In brief, this involved using Triton X-100 surfactant and glutaraldehyde to remove the cellular membrane and fix the cell before antibody labeling with Alexa Fluor dyes for SMLM. Single color microtubule imaging used rabbit anti-α-tubulin 1° antibody (1:500 in 5% BSA, Abcam ab18251) and Alexa Fluor 647 goat anti-rabbit IgG 2° antibody (1:200 in 5% BSA, Thermo Fisher A-21245). For two color imaging, rabbit anti-α-tubulin 1° antibody (1:500 in 5% BSA, Abcam ab18251) and Alexa Fluor 532 Goat anti-rabbit IgG 2° antibody (1:200 in 5% BSA, Thermo Fisher A-11009) were used to stain microtubules and Alexa Fluor 647 Phalloidin (Thermo Fisher, A-22287) was used to stain actin.

https://doi.org/10.1021/acsbiomedchemau.2c00086
ACS Bio Med Chem Au 2023, 3, 261−269

SOFI and SMLM Microtubule Width Analysis

SOFI and SMLM images were analyzed using Line Profiler,[35] extracting average fluorescence intensity cross sections of microtubules across the images, and analyzing their Gaussian fits to determine the standard deviation. Each cross section and Gaussian fit was observed, and those not tracing a single microtubule, such as fits of multiple microtubules or fluorescence peaks from only part of the microtubule, were discarded. The reported widths are an average of all remaining fitted cross sections.

■ ASSOCIATED CONTENT

Supporting Information

The Supporting Information is available free of charge at https://pubs.acs.org/doi/10.1021/acsbiomedchemau.2c00086.

Additional experimental details including varying plasmid transfection times for SOFI imaging, a control experiment comparing SMLM microtubule imaging of a cell with transfection of MAP4-N1-ffDronpa against a cell without. A box plot comparing microtubule diameters calculated from each microscopy, AFM microtubule intersection arrangement analysis and alternate targets for SOFI imaging (PDF)

Video 1: Example raw acquisition fluctuation data for SOFI (AVI)

Video 2: Example raw acquisition fluctuation data multi-tau SOFI (AVI)

■ AUTHOR INFORMATION

Corresponding Authors

Donna R. Whelan − *Department of Rural Clinical Sciences, La Trobe Institute for Molecular Science, La Trobe University, Bendigo 3552 Victoria, Australia*; Email: d.whelan@latrobe.edu.au

Toby D. M. Bell − *School of Chemistry, Monash University, Melbourne, Victoria 3800, Australia*; orcid.org/0000-0002-4570-5595; Email: toby.bell@monash.edu

Authors

Riley B. Hargreaves − *School of Chemistry, Monash University, Melbourne, Victoria 3800, Australia*

Sam Duwé − *Advanced Optical Microscopy Centre, Hasselt University, Diepenbeek 3590, Belgium*; orcid.org/0000-0003-3768-1877

Ashley M. Rozario − *Department of Rural Clinical Sciences, La Trobe Institute for Molecular Science, La Trobe University, Bendigo 3552 Victoria, Australia*

Alison M. Funston − *School of Chemistry, Monash University, Melbourne, Victoria 3800, Australia; ARC Centre of Excellence in Exciton Science, Monash University, Clayton, Victoria 3800, Australia*; orcid.org/0000-0002-4320-6434

Rico F. Tabor − *School of Chemistry, Monash University, Melbourne, Victoria 3800, Australia*; orcid.org/0000-0003-2926-0095

Peter Dedecker − *Department of Chemistry, KU Leuven, Leuven 3001, Belgium*

Complete contact information is available at: https://pubs.acs.org/10.1021/acsbiomedchemau.2c00086

Notes

The authors declare no competing financial interest.

■ ACKNOWLEDGMENTS

T.D.M.B. acknowledges support from the Australian Research Council (ARC) through a Discovery grant (DP170104477) and the National Health and Medical Research Council through an Ideas grant (1183478). R.F.T. is the recipient of the ARC Future Fellowship (FT160100191). D.R.W. acknowledges the Holsworth Biomedical Research Initiative under the auspices of the Bendigo Tertiary Education Anniversary Foundation and is the recipient of an Australian Research Council Discovery Early Career Research Award (DE200100584) funded by the Australian Government. A.M.F. acknowledges support from the Australian Research Council via the ARC Centre of Excellence in Exciton Science (CE170100026).

■ REFERENCES

(1) Whelan, D. R.; Bell, T. D. M. Super-resolution single-molecule localization microscopy: tricks of the trade. *journal of physical chemistry letters* **2015**, *6*, 374−382.

(2) Schnell, U.; Dijk, F.; Sjollema, K. A.; Giepmans, B. N. Immunolabeling artifacts and the need for live-cell imaging. *Nat. Methods* **2012**, *9*, 152−158.

(3) Whelan, D. R.; Bell, T. D. M. Correlative synchrotron fourier transform infrared spectroscopy and single molecule super resolution microscopy for the detection of composition and ultrastructure alterations in single cells. *ACS Chem. Biol.* **2015**, *10*, 2874−2883.

(4) Chudakov, D. M.; Matz, M. V.; Lukyanov, S.; Lukyanov, K. A. Fluorescent proteins and their applications in imaging living cells and tissues. *Physiol. Rev.* **2010**, *90*, 1103−1163.

(5) Wiedenmann, J.; Oswald, F.; Nienhaus, G. U. Fluorescent proteins for live cell imaging: opportunities, limitations, and challenges. *IUBMB life* **2009**, *61*, 1029−1042.

(6) Bálint, Š.; Verdeny Vilanova, I.; Sandoval Álvarez, Á.; Lakadamyali, M. Correlative live-cell and superresolution microscopy reveals cargo transport dynamics at microtubule intersections. *Proc. Natl. Acad. Sci. U. S. A.* **2013**, *110*, 3375−3380.

(7) Hargreaves, R. B.; Rozario, A. M.; McCoy, T. M.; Meaney, S. P.; Funston, A. M.; Tabor, R. F.; Whelan, D. R.; Bell, T. D. M. Optimising correlative super resolution and atomic force microscopies for investigating the cellular cytoskeleton. *Methods and Applications in Fluorescence* **2022**, *10*, 045005.

(8) Miranda, A.; Gómez-Varela, A. I.; Stylianou, A.; Hirvonen, L. M.; Sánchez, H.; De Beule, P. A. How did correlative atomic force microscopy and super-resolution microscopy evolve in the quest for unravelling enigmas in biology? *Nanoscale* **2021**, *13*, 2082−2099.

(9) Odermatt, P. D.; Shivanandan, A.; Deschout, H.; Jankele, R.; Nievergelt, A. P.; Feletti, L.; Davidson, M. W.; Radenovic, A.; Fantner, G. E. High-resolution correlative microscopy: bridging the gap between single molecule localization microscopy and atomic force microscopy. *Nano Lett.* **2015**, *15*, 4896−4904.

(10) Torra, J.; Viela, F.; Megías, D.; Sot, B.; Flors, C. Versatile Near-Infrared Super-Resolution Imaging of Amyloid Fibrils with the Fluorogenic Probe CRANAD-2. *Chemistry−A European Journal* **2022**, *28*, No. e202200026.

(11) Gómez-Varela, A. I.; Stamov, D. R.; Miranda, A.; Alves, R.; Barata-Antunes, C.; Dambournet, D.; Drubin, D. G.; Paiva, S.; De Beule, P. A. Simultaneous co-localized super-resolution fluorescence microscopy and atomic force microscopy: combined SIM and AFM platform for the life sciences. *Sci. Rep.* **2020**, *10*, 1−10.

(12) Harke, B.; Chacko, J. V.; Haschke, H.; Canale, C.; Diaspro, A. A novel nanoscopic tool by combining AFM with STED microscopy. *Optical Nanoscopy* **2012**, *1*, 3−6.

(13) Hirvonen, L. M.; Marsh, R. J.; Jones, G. E.; Cox, S. Combined AFM and super-resolution localisation microscopy: Investigating the structure and dynamics of podosomes. *European Journal of Cell Biology* **2020**, *99*, 151106.

(14) Bondia, P.; Jurado, R.; Casado, S.; Domínguez-Vera, J. M.; Gálvez, N.; Flors, C. Hybrid nanoscopy of hybrid nanomaterials. *Small* **2017**, *13*, 1603784.
(15) Godin, A. G.; Lounis, B.; Cognet, L. Super-resolution microscopy approaches for live cell imaging. *Biophysical journal* **2014**, *107*, 1777−1784.
(16) Zhao, W.; Zhao, S.; Li, L.; Huang, X.; Xing, S.; Zhang, Y.; Qiu, G.; Han, Z.; Shang, Y.; Sun, D.-e.; et al. Sparse deconvolution improves the resolution of live-cell super-resolution fluorescence microscopy. *Nature biotechnology* **2022**, *40*, 606−617.
(17) Stephan, T.; Roesch, A.; Riedel, D.; Jakobs, S. Live-cell STED nanoscopy of mitochondrial cristae. *Sci. Rep.* **2019**, *9*, 1−6.
(18) Shroff, H.; Galbraith, C. G.; Galbraith, J. A.; Betzig, E. Live-cell photoactivated localization microscopy of nanoscale adhesion dynamics. *Nat. Methods* **2008**, *5*, 417−423.
(19) Anzalone, A. V.; Chen, Z.; Cornish, V. W. Synthesis of photoactivatable azido-acyl caged oxazine fluorophores for live-cell imaging. *Chem. Commun.* **2016**, *52*, 9442−9445.
(20) Dertinger, T.; Colyer, R.; Iyer, G.; Weiss, S.; Enderlein, J. Fast, background-free, 3D super-resolution optical fluctuation imaging (SOFI). *Proc. Natl. Acad. Sci. U. S. A.* **2009**, *106*, 22287−22292.
(21) Vangindertael, J.; Camacho, R.; Sempels, W.; Mizuno, H.; Dedecker, P.; Janssen, K. An introduction to optical super-resolution microscopy for the adventurous biologist. *Methods and applications in fluorescence* **2018**, *6*, 022003.
(22) Dedecker, P.; Mo, G. C.; Dertinger, T.; Zhang, J. Widely accessible method for superresolution fluorescence imaging of living systems. *Proc. Natl. Acad. Sci. U. S. A.* **2012**, *109*, 10909−10914.
(23) Habuchi, S.; Ando, R.; Dedecker, P.; Verheijen, W.; Mizuno, H.; Miyawaki, A.; Hofkens, J. Reversible single-molecule photoswitching in the GFP-like fluorescent protein Dronpa. *Proc. Natl. Acad. Sci. U. S. A.* **2005**, *102*, 9511−9516.
(24) Duwé, S.; Dedecker, P. Optimizing the fluorescent protein toolbox and its use. *Curr. Opin. Biotechnol.* **2019**, *58*, 183−191.
(25) Duwé, S.; De Zitter, E.; Gielen, V.; Moeyaert, B.; Vandenberg, W.; Grotjohann, T.; Clays, K.; Jakobs, S.; Van Meervelt, L.; Dedecker, P. Expression-Enhanced Fluorescent Proteins Based on Enhanced Green Fluorescent Protein for Super-resolution Microscopy. *ACS Nano* **2015**, *9*, 9528−9541. PMID: 26308583
(26) Zeng, Z.; Chen, X.; Wang, H.; Huang, N.; Shan, C.; Zhang, H.; Teng, J.; Xi, P. Fast super-resolution imaging with ultra-high labeling density achieved by joint tagging super-resolution optical fluctuation imaging. *Sci. Rep.* **2015**, *5*, 1−7.
(27) Geissbuehler, S.; Sharipov, A.; Godinat, A.; Bocchio, N. L.; Sandoz, P. A.; Huss, A.; Jensen, N. A.; Jakobs, S.; Enderlein, J.; Gisou Van Der Goot, F.; et al. Live-cell multiplane three-dimensional super-resolution optical fluctuation imaging. *Nat. Commun.* **2014**, *5*, 1−7.
(28) Descloux, A.; Grußmayer, K.; Bostan, E.; Lukes, T.; Bouwens, A.; Sharipov, A.; Geissbuehler, S.; Mahul-Mellier, A.-L.; Lashuel, H.; Leutenegger, M.; et al. Combined multi-plane phase retrieval and super-resolution optical fluctuation imaging for 4D cell microscopy. *Nat. Photonics* **2018**, *12*, 165−172.
(29) Navikas, V.; Leitao, S. M.; Grussmayer, K. S.; Descloux, A.; Drake, B.; Yserentant, K.; Werther, P.; Herten, D.-P.; Wombacher, R.; Radenovic, A.; et al. Correlative 3D microscopy of single cells using super-resolution and scanning ion-conductance microscopy. *Nat. Commun.* **2021**, *12*, 1−9.
(30) Grußmayer, K.; Lukes, T.; Lasser, T.; Radenovic, A. Self-blinking dyes unlock high-order and multiplane super-resolution optical fluctuation imaging. *ACS Nano* **2020**, *14*, 9156−9165.
(31) Nienhaus, K.; Nienhaus, G. U. Fluorescent proteins for live-cell imaging with super-resolution. *Chem. Soc. Rev.* **2014**, *43*, 1088−1106.
(32) Duwé, S.; Vandenberg, W.; Dedecker, P. Live-cell monochromatic dual-label sub-diffraction microscopy by mt-pcSOFI. *Chem. Commun.* **2017**, *53*, 7242−7245.
(33) Rozario, A. M.; Duwé, S.; Elliott, C.; Hargreaves, R. B.; Moseley, G. W.; Dedecker, P.; Whelan, D. R.; Bell, T. D. Nanoscale characterization of drug-induced microtubule filament dysfunction using super-resolution microscopy. *BMC biology* **2021**, *19*, 1−16.
(34) Goodson, H. V.; Jonasson, E. M. Microtubules and microtubule-associated proteins. *Cold Spring Harbor perspectives in biology* **2018**, *10*, a022608.
(35) Zwettler, F. U.; Reinhard, S.; Gambarotto, D.; Bell, T. D.; Hamel, V.; Guichard, P.; Sauer, M. Molecular resolution imaging by post-labeling expansion single-molecule localization microscopy (Ex-SMLM). *Nat. Commun.* **2020**, *11*, 3388.
(36) Svitkina, T. The actin cytoskeleton and actin-based motility. *Cold Spring Harbor perspectives in biology* **2018**, *10*, a018267.
(37) Qi, J.; Liu, Y.; Chu, C.; Chen, X.; Zhu, W.; Shu, Y.; He, S.; Chai, R.; Zhong, G. A cytoskeleton structure revealed by super-resolution fluorescence imaging in inner ear hair cells. *Cell discovery* **2019**, *5*, 1−3.
(38) Joosten, B.; Willemse, M.; Fransen, J.; Cambi, A.; Van den Dries, K. Super-resolution correlative light and electron microscopy (SR-CLEM) reveals novel ultrastructural insights into dendritic cell podosomes. *Frontiers in immunology* **2018**, *9*, 1908.
(39) Nunnari, J.; Suomalainen, A. Mitochondria: in sickness and in health. *Cell* **2012**, *148*, 1145−1159.
(40) Edelstein, A.; Amodaj, N.; Hoover, K.; Vale, R.; Stuurman, N. Computer control of microscopes using μManager. *Current protocols in molecular biology* **2010**, *92*, 14−20.
(41) Dedecker, P.; Duwé, S.; Neely, R. K.; Zhang, J. Localizer: fast, accurate, open-source, and modular software package for super-resolution microscopy. *Journal of biomedical optics* **2012**, *17*, 126008.

https://doi.org/10.1021/acsbiomedchemau.2c00086
ACS Bio Med Chem Au 2023, 3, 261−269